

Flat-band solutions in D -dimensional decorated diamond and pyrochlore lattices: Reduction to molecular problem

Tomonari Mizoguchi,¹ Hosho Katsura,^{2,3,4} Isao Maruyama,⁵ and Yasuhiro Hatsugai¹

¹*Department of Physics, University of Tsukuba, Tsukuba, Ibaraki 305-8571, Japan**

²*Department of Physics, University of Tokyo, Hongo, Bunkyo-ku, Tokyo 113-0033, Japan*

³*Institute for Physics of Intelligence, The University of Tokyo,
7-3-1 Hongo, Bunkyo-ku, Tokyo 113-0033, Japan*

⁴*Trans-scale Quantum Science Institute, University of Tokyo, Bunkyo-ku, Tokyo 113-0033, Japan*

⁵*Department of Information and Systems Engineering,
Fukuoka Institute of Technology, Fukuoka 811-0295, Japan*

Flat-band models have been of particular interest from both fundamental aspects and realization in materials. Beyond the canonical examples such as Lieb lattices and line graphs, a variety of tight-binding models are found to possess flat bands. However, analytical treatment of dispersion relations is limited, especially when there are multiple flat bands with different energies. In this paper, we present how to determine flat-band energies and wave functions in tight-binding models on decorated diamond and pyrochlore lattices in generic dimensions $D \geq 2$. For two and three dimensions, such lattice structures are relevant to various organic and inorganic materials, and thus our method will be useful to analyze the band structures of these materials.

I. INTRODUCTION

Singular dispersions in band structures are the source of a variety of interesting phenomena in solid-state physics. One of the representative examples is a linear dispersion around the band crossing point, or the Dirac/Weyl point [1–3], which gives rise to various intriguing transport [4–6] and magnetic [7–10] phenomena. As such, Dirac/Weyl fermions in solids have been intensively pursued [1–3, 11–13]. Another example of singular dispersion is a flat band, which is a completely dispersionless band in the entire Brillouin zone. Studies of such band structure have been developed in various aspects, such as ferromagnetism [14–20], superconductivity [21–25], topological phenomena [26–42], and localization phenomena [43–48].

So far, various tight-binding models with flat bands have been explored [14, 49–58], and many insights on the model construction have been accumulated. It was also found that some flat-band models have large sublattice degrees of freedom, resulting in multiple flat bands with different energies [59–62]. In such models, it is not easy to obtain analytic expressions of dispersion relations since the Hamiltonians in momentum space are large matrices.

In this paper, we elucidate how to determine the flat-band energies analytically in a class of tight-binding models which can be obtained by decorating the bonds of a honeycomb lattice (in two dimensions) and a diamond lattice (in three dimensions), and their higher-dimensional analogs, $D \geq 4$; see Fig. 1 for the schematic figure of the two-dimensional model. Such lattice structures are of interest because they are known to be realized in various organic-based materials, such as graphene superstructures [63, 64], α -graphyne [65–68], and metal-

organic frameworks (MOFs) [68–71], as well as some inorganic materials [72, 73]. Recently, they were also discussed in the context of the square-root topological phases [74, 75]. We therefore expect that the determination of the flat-band energies is useful for band structure analysis and material design for these materials.

The key idea is to divide the Hamiltonian into two parts, which we term “linkers” and “linkages”. Importantly, the linkers and the linkages are not independent of each other since they share sites. Nevertheless, the flat-band energies can be obtained by solving the linkage Hamiltonian, and the corresponding wave function can be found such that the compatibility relations are respected on the shared sites. The momentum-independence of the eigenenergies originate from the fact that the linkage Hamiltonian can be regarded as that for an isolated “molecule” [76]. We find that the flat-band wave function

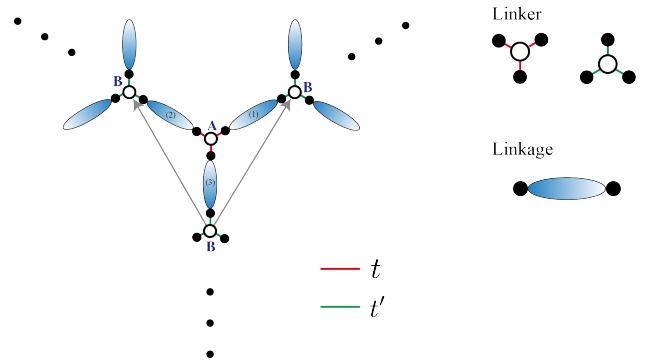


FIG. 1. A schematic of generic decorated diamond lattices. For clarity, we draw the case with $D = 2$. White dots stand for the vertices of the original diamond lattice, and gray arrows stand for the lattice vectors. Blue ellipses and black dots denote decorated parts. The schematics of linkers and linkages are also depicted. Note that the black dots belong to both linkers and linkages.

* mizoguchi@rhodia.ph.tsukuba.ac.jp

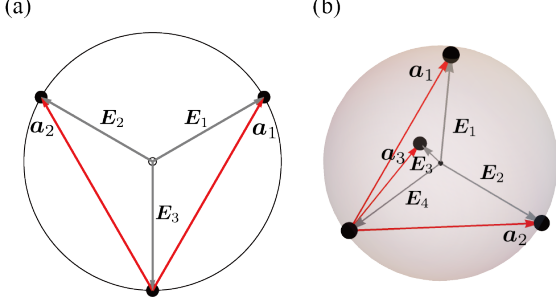


FIG. 2. Schematics of \mathbf{a}_j and \mathbf{E}_j of Eq. (1) for (a) two dimensions and (b) three dimensions.

of the D -dimensional decorated diamond lattice is given by the product of the wave function of the linkage and the flat-band wave function of D -dimensional pyrochlore lattice. We also shed light on another interesting band structure often seen in this class of lattices, namely, a multiple band touching at Γ point which occurs at specific choices of parameters.

The analog of the method described in this paper was previously applied to two-dimensional decorated kagome lattice [62], relevant to covalent organic frameworks (COFs) [60] as well as the cyclichgraphdiyne [77], where carbon atoms having different kinds of sp hybrid orbitals coexist and form a crystal. Here we emphasize that this method yields not only the energies of the flat bands but also their wave functions, which was not addressed in the previous work. Therefore, for completeness, we also explain the method for obtaining flat-band energies and eigenstates for the d -dimensional decorated pyrochlore lattice.

II. FLAT-BAND SOLUTIONS FOR D -DIMENSIONAL DECORATED DIAMOND LATTICES

A. Model

Consider a diamond lattice in D dimensions with $D \geq 2$ [51, 81–83]. The lattice vectors are given as [51]

$$\mathbf{a}_j = \mathbf{E}_j - \mathbf{E}_{D+1}, \quad (1)$$

where $j = 1, \dots, D$ and the vectors $\mathbf{E}_1, \dots, \mathbf{E}_{D+1}$ are the vertices of the D -simplex; see Fig. 2 for the schematics of $D = 2, 3$. We set the coordinates of two sublattices of the D -dimensional diamond lattice (for $D = 2$, see the white dots of Fig. 1) as

$$\mathbf{r}_A = \frac{1}{D+1} \sum_{j=1}^D \mathbf{a}_j, \quad (2)$$

and

$$\mathbf{r}_B = \mathbf{0}. \quad (3)$$

Now, let us consider the decorated lattices of D -dimensional diamonds, shown in Fig. 1. Namely, we decorate the nearest-neighbor (NN) bonds of the diamond lattices, obeying the following rules:

- The sublattices A and B of the original diamond lattice are, respectively, connected to $D+1$ sites with the same hoppings (red and green bonds in Fig. 1).
 - The decorated objects are the same for all the NN bonds.
- For later use, let us clarify some terminologies:
- We call a set of $D+2$ sites, composed of one site placed on the original diamond lattice and the other $D+1$ sites connected to that site, a “linker”.
 - We call a decorated part on each edge of the diamond lattice a “linkage”.

It is worth noting that the black dots in Fig. 1 belong to both a linker and a linkage.

On this class of lattices, we consider the following Hamiltonian in \mathbf{k} -space, which is in general written as a $[(D+1)q+2]$ -dimensional matrix:

$$\mathcal{H}_{\mathbf{k}} = \begin{pmatrix} U_A & t\mathbf{x}_q^T & t\mathbf{x}_q^T & \cdots & \cdots & 0 \\ t\mathbf{x}_q & \mathcal{H}_{\text{linkage}}^{(1)} & \mathcal{O}_q & \cdots & \mathcal{O}_q & t'e^{i\mathbf{k}\cdot\mathbf{a}_1}\mathbf{y}_q \\ t\mathbf{x}_q & \mathcal{O}_q & \mathcal{H}_{\text{linkage}}^{(2)} & \ddots & \vdots & t'e^{i\mathbf{k}\cdot\mathbf{a}_2}\mathbf{y}_q \\ \vdots & \vdots & \ddots & \ddots & \mathcal{O}_q & \vdots \\ t\mathbf{x}_q & \mathcal{O}_q & \cdots & \mathcal{O}_q & \mathcal{H}_{\text{linkage}}^{(D+1)} & t'\mathbf{y}_q \\ 0 & t'e^{-i\mathbf{k}\cdot\mathbf{a}_1}\mathbf{y}_q^T & t'e^{-i\mathbf{k}\cdot\mathbf{a}_2}\mathbf{y}_q^T & \cdots & t'\mathbf{y}_q^T & U_B \end{pmatrix}, \quad (4)$$

where \mathbf{x}_q and \mathbf{y}_q are q -component column vectors defined as $\mathbf{x}_q := (1, 0, \dots, 0)^T$ and $\mathbf{y}_q := (0, \dots, 1)^T$, respectively, and \mathcal{O}_q stands for the $q \times q$ zero matrix. The parameters, U_A and U_B , are on-site potentials for sublattices A and B, respectively; t and t' are, respectively, the transfer integrals assigned on the bonds connecting the decorated part with the sublattices A and B.

For later use, we define two $(D+1)$ -component row vectors, $\psi^{(1)\dagger}$ and $\psi_k^{(2)\dagger}$, which have the forms:

$$\psi^{(1)\dagger} = (1, 1, \dots, 1), \quad (5a)$$

and

$$\psi_k^{(2)\dagger} = (e^{-i\mathbf{k} \cdot \mathbf{a}_1}, \dots, e^{-i\mathbf{k} \cdot \mathbf{a}_D}, 1), \quad (5b)$$

and the multiplet composed of these two vectors [78]:

$$\Psi_k^\dagger = \begin{pmatrix} \psi^{(1)\dagger} \\ \psi_k^{(2)\dagger} \end{pmatrix}. \quad (6)$$

The matrix $\mathcal{H}_{\text{linkage}}^{(j)}$ in Eq. (4) can be regarded as a Hamiltonian of an isolated “molecule”. In the present case, we assume that all the linkages have the same structure, i.e., the following holds:

$$\mathcal{H}_{\text{linkage}}^{(1)} = \mathcal{H}_{\text{linkage}}^{(2)} = \dots = \mathcal{H}_{\text{linkage}}^{(D+1)} = \mathcal{H}_{\text{linkage}}. \quad (7)$$

B. Derivation of flat-band solution

This type of models possess multiple flat bands with different energies [63, 68, 72]. Remarkably, if the number of decorated sites on each bond is q , there exist q flat bands with different energies. More precisely, in the D -dimensional model, each flat band has $(D-1)$ -fold degeneracy, thus the number of flat bands is equal to $(D-1)q$.

In general, analytic solutions of the dispersion relations in this class of models are hard to obtain, since the size of the Hamiltonian matrix is large. Nevertheless, we can obtain the eigenvalues and eigenvectors of the flat bands as follows. Let $\boldsymbol{\lambda}_{\text{linker}, \mathbf{k}}$ be a $(D+1)$ -component column vector, which satisfies

$$\Psi_k^\dagger \boldsymbol{\lambda}_{\text{linker}, \mathbf{k}} = \begin{pmatrix} 0 \\ 0 \end{pmatrix}. \quad (8)$$

As Ψ_k^\dagger is the $2 \times (D+1)$ matrix, there are $D-1$ independent solutions of $\boldsymbol{\lambda}_{\text{linker}, \mathbf{k}}$. Only at the Γ point (i.e., $\mathbf{k} = \mathbf{0}$), the rank of Ψ_k^\dagger is reduced by one as $\psi^{(1)} = \psi_k^{(2)}$ holds, which results in the increase of the number of solutions from $D-1$ to D . We note that $\boldsymbol{\lambda}_{\text{linker}, \mathbf{k}}$ corresponds to the flat-band eigenvector of the D -dimensional pyrochlore lattice [51].

To find the flat-band solution, we employ a notion of “intertwiner” [79, 80]. Before going to the concrete problem, we briefly address a generic argument. Let A and G be Hermitian matrices with different sizes. It is known

that A and G have common eigenvalues if these matrices satisfy

$$AC = CG, \quad (9)$$

with C being a non-square matrix. The matrix C is called the “intertwiner”. A simple proof of this statement is as follows. Let ϕ be an eigenvector of G with eigenvalue ε . Then, one finds that $C\phi$ is an eigenvector of A with eigenvalue ε (unless ϕ belongs to the kernel of C), because

$$A(C\phi) = CG\phi = \varepsilon(C\phi). \quad (10)$$

Turning to the present model, we can explicitly construct the intertwiner C_k which is $[(D+1)q+2] \times q$ matrix and satisfies

$$\mathcal{H}_k C_k = C_k \mathcal{H}_{\text{linkage}}. \quad (11)$$

Its form is given as

$$C_k = \begin{pmatrix} \mathbf{0}_q^T \\ [\boldsymbol{\lambda}_{\text{linker}, \mathbf{k}}]_1 I_q \\ \vdots \\ [\boldsymbol{\lambda}_{\text{linker}, \mathbf{k}}]_{D+1} I_q \\ \mathbf{0}_q^T \end{pmatrix}, \quad (12)$$

where $\mathbf{0}_q$ stands for the q -component column zero vector and $[\boldsymbol{\lambda}_{\text{linker}, \mathbf{k}}]_j$ is the j -th component of $\boldsymbol{\lambda}_{\text{linker}, \mathbf{k}}$. Therefore, the eigenvalues of $\mathcal{H}_{\text{linkage}}$ are also those of \mathcal{H}_k . As $\mathcal{H}_{\text{linkage}}$ is \mathbf{k} -independent, the eigenvalues obtained as such naturally form flat bands. Equation (11) also leads to the flat-band wave function. Let $\phi_{\text{linkage}, n}$ be a q -component vector which is the n th eigenvector of $\mathcal{H}_{\text{linkage}}$. It satisfies

$$\mathcal{H}_{\text{linkage}} \phi_{\text{linkage}, n} = \varepsilon_{\text{linkage}, n} \phi_{\text{linkage}, n} \quad (13)$$

with $\varepsilon_{\text{linkage}, n}$ being the eigenvalue. Then, the flat-band eigenvector $\varphi_{k, n}$, written as

$$\varphi_{k, n} = \begin{pmatrix} \varphi_{A, \mathbf{k}, n} \\ \varphi_{1, \mathbf{k}, n} \\ \vdots \\ \varphi_{(D+1)q, \mathbf{k}, n} \\ \varphi_{B, \mathbf{k}, n} \end{pmatrix}, \quad (14)$$

is given as

$$\varphi_{k, n} = \frac{1}{\mathcal{N}_k} C_k \phi_{\text{linkage}, n}, \quad (15)$$

where \mathcal{N}_k is the normalization constant. More concretely, the components of $\varphi_{k, n}$ are given as

$$\varphi_{A, \mathbf{k}, n} = \varphi_{B, \mathbf{k}, n} = 0, \quad (16)$$

and

$$\varphi_{q(j-1)+m, \mathbf{k}, n} = \frac{1}{\mathcal{N}_k} [\boldsymbol{\lambda}_{\text{linker}, \mathbf{k}}]_j [\phi_{\text{linkage}, n}]_m \quad (17)$$

with $j = 1, \dots, D + 1$ and $m = 1, \dots, q$. Equation (17) indicates that the flat-band wave function of the D -dimensional decorated diamond lattice is given by the product of the linkage's wave function and the flat-band wave function of D -dimensional pyrochlore lattice.

In the next section, we elucidate how this construction actually works by showing specific examples.

III. EXAMPLES

In this section, we demonstrate that the aforementioned method works for decorated diamond lattices in $D = 2, 3$ and 4. Although our formulation is applicable to generic types of decoration patterns, we mainly focus on the model where the chain-type structure is inserted between the neighboring sites of the diamond lattices. (We present an example of the non-chain-type decorating sites for $D = 2$; see Fig. 4.) The motivation to focus on these models is that, for $D = 2, 3$, they are known to be relevant to MOFs such as DCBP₃Co₂ and DCA₃Co₂ [71], α -graphyne [65–68], and TaS₂ [72, 73]. (DCBP and DCA stand for dicyanobiphenyl and dicyanoanthracene, respectively). As for $D = 4$, some recent works addressed the four-dimensional diamond lattice [81–83] as a canonical example of four-dimensional Dirac fermions on lattice models. In this context, the decorated four-dimensional diamond lattice is an interesting extension of it where Dirac fermions and flat bands coexist.

A. Two dimensions: Decorated honeycomb lattice

Consider a decorated honeycomb lattice model with q sites on each edge of hexagons [Fig. 3(a)]. The specific form of the Hamiltonian is given by substituting $t = t_1$, $t' = t_{q+1}$, and

$$\mathcal{H}_{\text{linkage}}^{\text{DH}} = \begin{pmatrix} U_1 & t_2 & 0 & \cdots & \cdots & 0 \\ t_2 & U_2 & t_3 & \cdots & \cdots & 0 \\ 0 & t_3 & U_3 & \cdots & \cdots & 0 \\ \vdots & & & \ddots & & \vdots \\ 0 & \cdots & \cdots & \cdots & U_{q-1} & t_q \\ 0 & \cdots & \cdots & \cdots & t_q & U_q \end{pmatrix} \quad (18)$$

into Eq. (4). The row vectors $\psi^{\text{DH}(1)\dagger}$ and $\psi_{\mathbf{k}}^{\text{DH}(2)\dagger}$ are given as

$$\psi^{\text{DH}(1)\dagger} = (1, 1, 1), \quad (19)$$

$$\psi_{\mathbf{k}}^{\text{DH}(2)\dagger} = (e^{-i\mathbf{k} \cdot \mathbf{a}_1^{\text{DH}}}, e^{-i\mathbf{k} \cdot \mathbf{a}_2^{\text{DH}}}, 1). \quad (20)$$

The vector $\lambda_{\text{linker}, \mathbf{k}}^{\text{DH}}$ is obtained as

$$\lambda_{\text{linker}, \mathbf{k}}^{\text{DH}} = \begin{pmatrix} 1 - e^{-i\mathbf{k} \cdot \mathbf{a}_2^{\text{DH}}} \\ e^{-i\mathbf{k} \cdot \mathbf{a}_1^{\text{DH}}} - 1 \\ e^{-i\mathbf{k} \cdot \mathbf{a}_2^{\text{DH}}} - e^{-i\mathbf{k} \cdot \mathbf{a}_1^{\text{DH}}} \end{pmatrix}. \quad (21)$$

Then, the flat-band energies are equal to the eigenvalues of $\mathcal{H}_{\text{linkage}}^{\text{DH}}$, and the corresponding wave functions are given in the form of Eq. (17).

In Figs. 3(d)-(f), we plot the band structures for $q = 3$ with several sets of parameters. In all cases, there are three flat bands, whose energies are indeed equal to $\varepsilon_{\text{linkage}, n}$.

It is also interesting to find that the triple band touching, where the flat band penetrates the band touching point of dispersive bands, occurs at Γ point in some cases [e.g., $\varepsilon = 0$ in Fig. 3(d)]. In what follows, we elucidate the condition for the triple band touching, by explicitly derive the eigenenergies at Γ point.

Before proceeding further, we remark that any of the flat bands touches the dispersive band at Γ point regardless of the parameters. This is because of the rank reduction of $\Psi_{\mathbf{k}}^\dagger$, which we have mentioned in Sec. II A. Therefore, from the above derivation of the flat-band energies, we have already obtained $2q$ eigenenergies out of $3q + 2$ at Γ point, thus we need to derive the remaining $q + 2$ eigenenergies.

For the derivation of the eigenenergies at Γ point, we first point out that the remaining eigenstates have three-fold rotational symmetries centered at A site and B site. Therefore, the wave function satisfies

$$\varphi_m = \varphi_{m+q} = \varphi_{m+2q}, \quad (22)$$

for $m = 1, \dots, q$. Substituting (22) into the Schrödinger equation, we find that it is reduced to the eigenvalue equation of the following $(q + 2) \times (q + 2)$ matrix:

$$\mathcal{X} = \begin{pmatrix} U_A & 3t_1 & 0 & \cdots & \cdots & 0 \\ t_1 & U_1 & t_2 & \cdots & \cdots & 0 \\ 0 & t_2 & U_2 & \cdots & \cdots & 0 \\ \vdots & & & \ddots & & \vdots \\ 0 & \cdots & \cdots & \cdots & U_q & t_{q+1} \\ 0 & \cdots & \cdots & \cdots & 3t_{q+1} & U_B \end{pmatrix}. \quad (23)$$

Clearly, \mathcal{X} is a non-Hermitian matrix, since $(1, 2)$ and $(2, 1)$ components are different and so are $(q - 1, q)$ and $(q, q - 1)$ components. Nevertheless, all the eigenvalues of \mathcal{X} are real, since there exists a similarity transformation such that \mathcal{X} is transformed into the Hermitian matrix:

$$P^{-1} \mathcal{X} P = \tilde{\mathcal{H}}, \quad (24)$$

with $P = \text{diag}(\sqrt{3}, 1, \dots, 1, \sqrt{3})$ and

$$\tilde{\mathcal{H}} = \begin{pmatrix} U_A & \sqrt{3}t_1 & 0 & \cdots & \cdots & 0 \\ \sqrt{3}t_1 & U_1 & t_2 & \cdots & \cdots & 0 \\ 0 & t_2 & U_2 & \cdots & \cdots & 0 \\ \vdots & & & \ddots & & \vdots \\ 0 & \cdots & \cdots & \cdots & U_q & \sqrt{3}t_{q+1} \\ 0 & \cdots & \cdots & \cdots & \sqrt{3}t_{q+1} & U_B \end{pmatrix}. \quad (25)$$

Then, denoting the eigenvalues of $\tilde{\mathcal{H}}$ as $\varepsilon_{n'}^{\text{Disp.}}(t_1, t_2, t_3, \dots, t_q, t_{q+1}; U_A, U_1, U_2, \dots, U_q, U_B)$ with

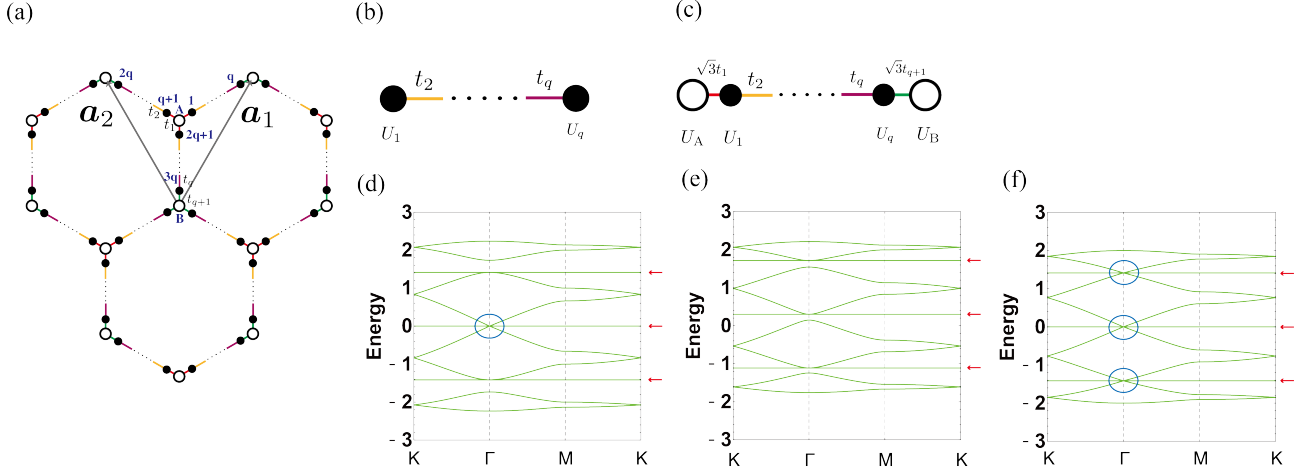


FIG. 3. (a) A decorated honeycomb lattice with q sites on edges of hexagons. The lattice vectors are $\mathbf{a}_1^{\text{DH}} = \left(\frac{1}{2}, \frac{\sqrt{3}}{2}\right)$ and $\mathbf{a}_2^{\text{DH}} = \left(-\frac{1}{2}, \frac{\sqrt{3}}{2}\right)$. Schematics of the Hamiltonians of the chain-like molecules corresponding to (b) $\mathcal{H}_{\text{chain}}$ and (c) $\tilde{\mathcal{H}}$. The band structures for $q = 3$ for (d) $(t_1, t_2, t_3, t_4, U_A, U_1, U_2, U_3, U_B) = (1, 1, 1, 1, 0, 0, 0, 0, 0)$, (e) $(0.8, 1, 1, 0.8, 0, 0.3, 0.3, 0.3, 0)$, and (f) $\left(\sqrt{\frac{2}{3}}, 1, 1, \sqrt{\frac{2}{3}}, 0, 0, 0, 0, 0\right)$. Red arrows point to the flat bands, and the blue circles represent the triple band touchings. The coordinates of the high-symmetry points in the first Brillouin zone are $\Gamma = (0, 0)$, $K = \left(\frac{4\pi}{3}, 0\right)$, and $M = \left(\pi, \frac{\pi}{\sqrt{3}}\right)$.

$n' = 1, \dots, q + 2$, we can write down the condition for the triple band touching as

$$\begin{aligned} & \varepsilon_{\text{linkage}, n}(t_2, t_3, \dots, t_q, U_1, U_2, \dots, U_q) \\ &= \varepsilon_{n'}^{\text{Disp.}}(t_1, t_2, t_3, \dots, t_q, t_{q+1}, U_A, U_1, U_2, \dots, U_q, U_B), \end{aligned} \quad (26)$$

for some $n = 1, \dots, q$ and $n' = 1, \dots, q + 2$.

For the special case when both $\mathcal{H}_{\text{linkage}}$ and $\tilde{\mathcal{H}}$ are chi-

ral symmetric (i.e., $U_A = U_B = U_1 = \dots = U_q = 0$), and q is an odd number, both $\mathcal{H}_{\text{linkage}}$ and $\tilde{\mathcal{H}}$ have a zero eigenvalue, thus the triple band touching at $\varepsilon = 0$ is guaranteed. Indeed, Fig. 3(d) is an example of such a case. As a further interesting case, we show an example where all of the flat bands exhibit the triple band touching in Fig. 3(f). In fact, such a set of parameters can be found by using the wisdom of the Dynkin diagrams; see Appendix A for details.

Before closing this subsection, we present two additional examples beyond the model discussed so far. The first one is the case where the decoration sites are not aligned in a chain, as depicted in Fig. 4(a). Even in this

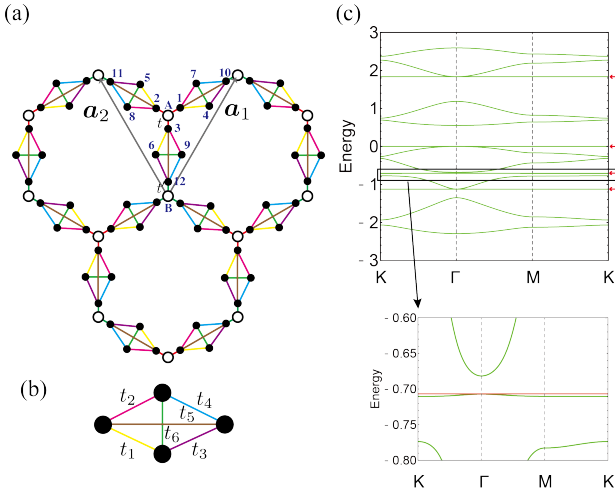


FIG. 4. (a) A decorated honeycomb lattice with four decorating sites, shaped in the rhombus, at each edge. (b) Schematic figure of the four-site molecule whose eigenenergies are equal to the flat-band energies. (c) The band structure for $(t, t', t_1, t_2, t_3, t_4, t_5, t_6) = (1, 0.9, 0.4, 0.5, 0.6, 0.3, 1.1, 0.7)$. The on-site potentials are zero. Red arrows point to the flat bands.

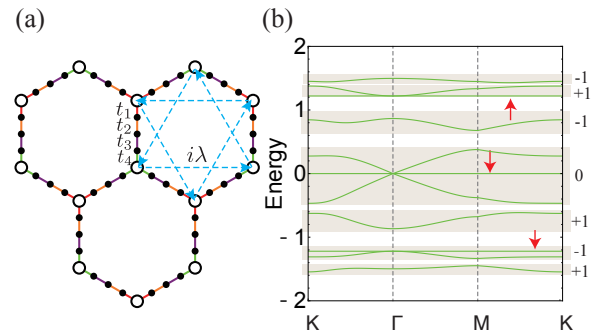


FIG. 5. (a) Schematic figure of \mathcal{H}'_k of Eq. (27). Blue dashed arrows represent the complex hoppings. (b) Band structure for the model of the panel (a) with $(t_1, t_2, t_3, t_4, \lambda) = (0.5, 0.7, 1.0, 0.5, 0.1)$. The on-site potentials are zero. The numbers beside the bands indicate the Chern numbers, which are calculated for the set of bands included in the same shade. Red arrows point the flat bands.

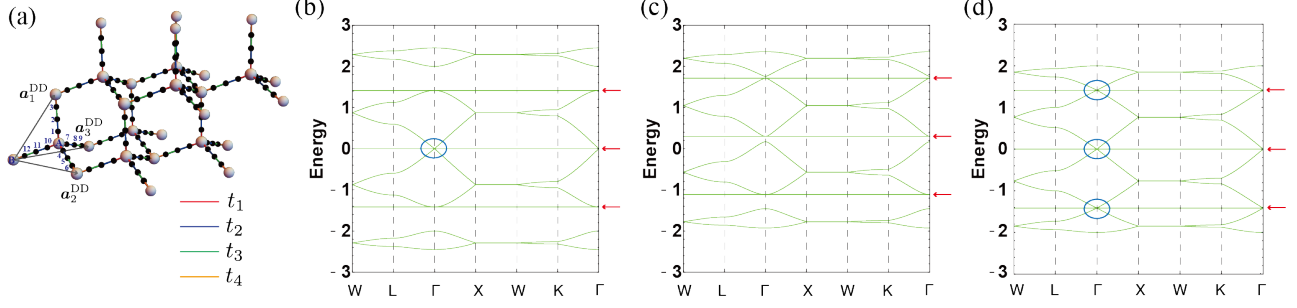


FIG. 6. (a) A decorated diamond lattice with three sites on NN bonds of a diamond lattice. The lattice vectors are $\mathbf{a}_1^{\text{DD}} = (0, \frac{1}{2}, \frac{1}{2})$, $\mathbf{a}_2^{\text{DD}} = (\frac{1}{2}, 0, \frac{1}{2})$, and $\mathbf{a}_3^{\text{DD}} = (\frac{1}{2}, \frac{1}{2}, 0)$. The band structures for (b) $(t_1, t_2, t_3, t_4, U_A, U_1, U_2, U_3, U_B) = (1, 1, 1, 1, 0, 0, 0, 0, 0)$, (c) $(0.8, 1, 1, 0.8, 0, 0.3, 0.3, 0.3, 0)$, and (d) $(\frac{1}{\sqrt{2}}, 1, 1, \frac{1}{\sqrt{2}}, 0, 0, 0, 0, 0)$. Red arrows point to the flat bands, and the blue circle represents the quadruple band touching. The coordinates of the high-symmetry points in the first Brillouin zone are $\Gamma = (0, 0, 0)$, $W = (\pi, 0, 2\pi)$, $L = (\pi, \pi, \pi)$, $X = (0, 0, 2\pi)$ and $K = (\frac{3\pi}{2}, 0, \frac{3\pi}{2})$.

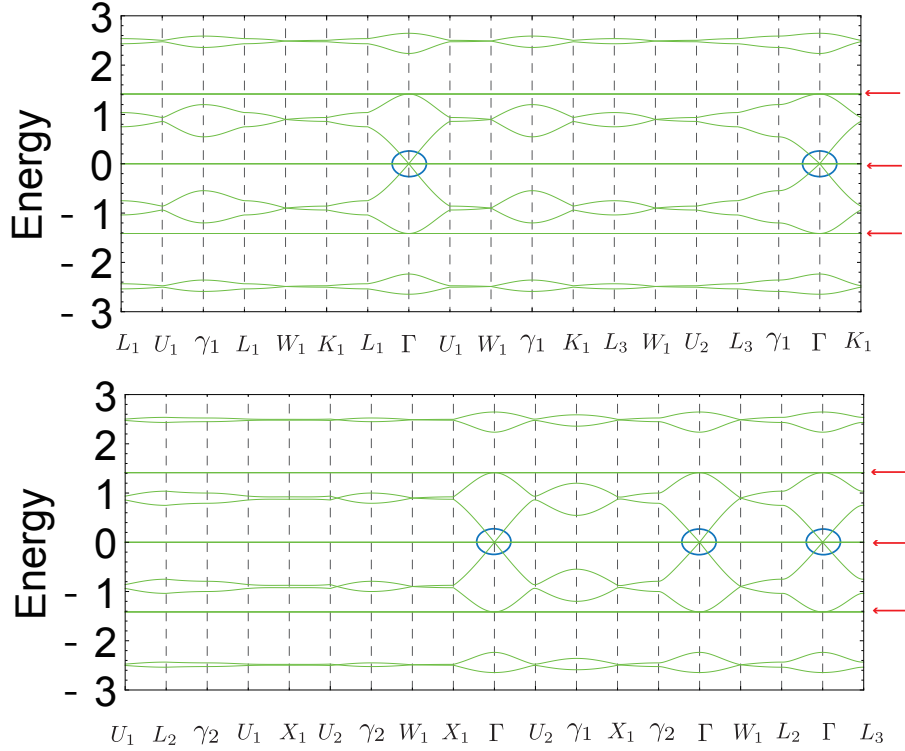


FIG. 7. The band structure of the decorated four-dimensional diamond lattice with $q = 3$. The parameters are set as $(t_1, t_2, t_3, t_4, U_A, U_1, U_2, U_3, U_B) = (1, 1, 1, 1, 0, 0, 0, 0, 0)$. Upper and lower panels are for different high-symmetry lines. Red arrows point to the flat bands, and blue circles represent the quintuple band touchings.

case, the flat-band energies are obtained by solving the eigenvalue problem of the “molecule” formed by the decorating sites [Fig. 4(b)]. Indeed, we find four flat bands in Fig. 4(c), whose energies are equal to those for Fig. 4(b).

The second example is the Chern insulator on the decorated honeycomb lattice. As we have seen, the flat band

wave functions have amplitudes only on the linkages. Therefore, if one modifies the model such that the additional term acts only on the vertices of the honeycomb lattice, the model still hosts the exact flat band. Keeping this in mind, we add the complex hopping among the vertices of the honeycomb lattice to $\mathcal{H}_k^{\text{DH}}$ of Eq. (18), to

make the dispersive bands topological [see Fig. 5 (a) for the schematic figure]. Specifically, the additional term, $\mathcal{H}'_{\mathbf{k}}$, has the same form as the Haldane model [84]:

$$\mathcal{H}'_{\mathbf{k}} = \sum_{\mathbf{k}} 2\lambda M_{\mathbf{k}} \left(c_{\mathbf{k},A}^\dagger c_{\mathbf{k},A} - c_{\mathbf{k},B}^\dagger c_{\mathbf{k},B} \right) \quad (27)$$

with $M_{\mathbf{k}} = \sin \mathbf{k} \cdot \mathbf{a}_1^{\text{DH}} - \sin \mathbf{k} \cdot \mathbf{a}_2^{\text{DH}} - \sin \mathbf{k} \cdot (\mathbf{a}_1^{\text{DH}} - \mathbf{a}_2^{\text{DH}})$. The band structure for a representative set of parameters with $q = 3$ is shown in Fig. 5(b). We compute the Chern number numerically by using the method of Ref. 85. Clearly, the exact flat bands survive and some of the dispersive bands acquire the non-trivial Chern numbers. Further, some of the flat bands have quadratic band touching with topologically-nontrivial dispersive bands. Similar band structure was seen in the kagome-lattice model discussed in Ref. 40.

B. Three and four dimensions

The same method is applicable to the case of three- and four-dimensional decorated honeycomb lattice with q sites on each edge. In such models, the flat-band energies are given by the eigenenergies of $\mathcal{H}_{\text{linkage}}$, regardless of the dimensionality.

Figures 6 and 7 show the resulting band structures for three dimensions and four dimensions, respectively, with $q = 3$. For the coordinates of the high-symmetry points in the four-dimensional Brillouin zone, we follow Ref. [83]; see Appendix B. We note that the degeneracy of each flat band is two (three) for $D = 3$ ($D = 4$). Correspondingly, the band touchings at Γ point denoted by the blue circles in Figs. 6 and 7 have $D + 1$ -fold degeneracy for the D -dimensional system.

IV. D -DIMENSIONAL DECORATED PYROCHLORE LATTICES

In this section, we discuss yet another series of multiple flat-band systems, namely, D -dimensional decorated pyrochlore lattices. For concreteness, we consider the three-dimensional decorated pyrochlore model with one decorating site between neighboring tetrahedra [Fig. 8(a)]. Extension to generic dimensions and generic forms of

decoration is straightforward. (For instance, the result for the two-dimensional analog is presented in the prior work [62].) We note that this type of lattice structure, both in two and three dimensions, has various material realizations, mainly in organic systems [60–62, 77, 86–88].

We consider the lattice of Fig. 8(a). Three lattice vectors are in common with the decorated diamond lattice. The Hamiltonian is the 12×12 matrix given as

$$\mathcal{H}_{\mathbf{k}}^{\text{DP}} = \begin{pmatrix} \tilde{\mathcal{H}}_{\text{linkage}}^{\text{DP}} & V_{\mathbf{k},(1,2)} & V_{\mathbf{k},(1,3)} & V_{\mathbf{k},(1,4)} \\ V_{\mathbf{k},(2,1)} & \tilde{\mathcal{H}}_{\text{linkage}}^{\text{DP}} & V_{\mathbf{k},(2,3)} & V_{\mathbf{k},(2,4)} \\ V_{\mathbf{k},(3,1)} & V_{\mathbf{k},(3,4)} & \tilde{\mathcal{H}}_{\text{linkage}}^{\text{DP}} & V_{\mathbf{k},(3,4)} \\ V_{\mathbf{k},(4,1)} & V_{\mathbf{k},(4,2)} & V_{\mathbf{k},(4,3)} & \tilde{\mathcal{H}}_{\text{linkage}}^{\text{DP}} \end{pmatrix}, \quad (28)$$

where

$$\tilde{\mathcal{H}}_{\text{linkage}}^{\text{DP}} = \begin{pmatrix} 0 & t_3 & 0 \\ t_3 & 0 & t_4 \\ 0 & t_4 & 0 \end{pmatrix}, \quad (29)$$

and

$$V_{\mathbf{k},(i,j)} = \begin{pmatrix} t_1 & 0 & 0 \\ 0 & 0 & 0 \\ 0 & 0 & t_2 e^{-i\mathbf{k} \cdot (\mathbf{a}_i^{\text{DD}} - \mathbf{a}_j^{\text{DD}})} \end{pmatrix} \quad (30)$$

with $\mathbf{a}_4^{\text{DD}} = (0, 0, 0)$.

To obtain the flat band solution, we again give the intertwiner explicitly. In the present model, we have

$$\mathcal{H}_{\mathbf{k}}^{\text{DP}} C_{\mathbf{k}} = C_{\mathbf{k}} \mathcal{H}_{\text{linkage}}^{\text{DP}}, \quad (31)$$

where

$$C_{\mathbf{k}} = \begin{pmatrix} [\lambda_{\text{linker},\mathbf{k}}]_1 I_3 \\ [\lambda_{\text{linker},\mathbf{k}}]_2 I_3 \\ [\lambda_{\text{linker},\mathbf{k}}]_3 I_3 \\ [\lambda_{\text{linker},\mathbf{k}}]_4 I_3 \end{pmatrix}, \quad (32)$$

and

$$\mathcal{H}_{\text{linkage}}^{\text{DP}} = \begin{pmatrix} -t_1 & t_3 & 0 \\ t_3 & 0 & t_4 \\ 0 & t_4 & -t_2 \end{pmatrix}, \quad (33)$$

where $\lambda_{\text{linker},\mathbf{k}}$ is the same as that for the decorated diamond model. Note that the left-hand side of Eq. (31) becomes

$$\begin{aligned} \mathcal{H}_{\mathbf{k}}^{\text{DP}} C_{\mathbf{k}} &= \begin{pmatrix} \tilde{\mathcal{H}}_{\text{linkage}}^{\text{DP}} & V_{\mathbf{k},(1,2)} & V_{\mathbf{k},(1,3)} & V_{\mathbf{k},(1,4)} \\ V_{\mathbf{k},(2,1)} & \tilde{\mathcal{H}}_{\text{linkage}}^{\text{DP}} & V_{\mathbf{k},(2,3)} & V_{\mathbf{k},(2,4)} \\ V_{\mathbf{k},(3,1)} & V_{\mathbf{k},(3,4)} & \tilde{\mathcal{H}}_{\text{linkage}}^{\text{DP}} & V_{\mathbf{k},(3,4)} \\ V_{\mathbf{k},(4,1)} & V_{\mathbf{k},(4,2)} & V_{\mathbf{k},(4,3)} & \tilde{\mathcal{H}}_{\text{linkage}}^{\text{DP}} \end{pmatrix} \begin{pmatrix} [\lambda_{\text{linker},\mathbf{k}}]_1 I_3 \\ [\lambda_{\text{linker},\mathbf{k}}]_2 I_3 \\ [\lambda_{\text{linker},\mathbf{k}}]_3 I_3 \\ [\lambda_{\text{linker},\mathbf{k}}]_4 I_3 \end{pmatrix} \\ &= \begin{pmatrix} [\lambda_{\text{linker},\mathbf{k}}]_1 \tilde{\mathcal{H}}_{\text{linkage}}^{\text{DP}} + [\lambda_{\text{linker},\mathbf{k}}]_2 V_{\mathbf{k},(1,2)} + [\lambda_{\text{linker},\mathbf{k}}]_3 V_{\mathbf{k},(1,3)} + [\lambda_{\text{linker},\mathbf{k}}]_4 V_{\mathbf{k},(1,4)} \\ [\lambda_{\text{linker},\mathbf{k}}]_2 \tilde{\mathcal{H}}_{\text{linkage}}^{\text{DP}} + [\lambda_{\text{linker},\mathbf{k}}]_1 V_{\mathbf{k},(2,1)} + [\lambda_{\text{linker},\mathbf{k}}]_3 V_{\mathbf{k},(2,3)} + [\lambda_{\text{linker},\mathbf{k}}]_4 V_{\mathbf{k},(2,4)} \\ [\lambda_{\text{linker},\mathbf{k}}]_3 \tilde{\mathcal{H}}_{\text{linkage}}^{\text{DP}} + [\lambda_{\text{linker},\mathbf{k}}]_1 V_{\mathbf{k},(3,1)} + [\lambda_{\text{linker},\mathbf{k}}]_2 V_{\mathbf{k},(3,2)} + [\lambda_{\text{linker},\mathbf{k}}]_4 V_{\mathbf{k},(3,4)} \\ [\lambda_{\text{linker},\mathbf{k}}]_4 \tilde{\mathcal{H}}_{\text{linkage}}^{\text{DP}} + [\lambda_{\text{linker},\mathbf{k}}]_1 V_{\mathbf{k},(4,1)} + [\lambda_{\text{linker},\mathbf{k}}]_2 V_{\mathbf{k},(4,2)} + [\lambda_{\text{linker},\mathbf{k}}]_3 V_{\mathbf{k},(4,3)} \end{pmatrix}. \end{aligned} \quad (34)$$

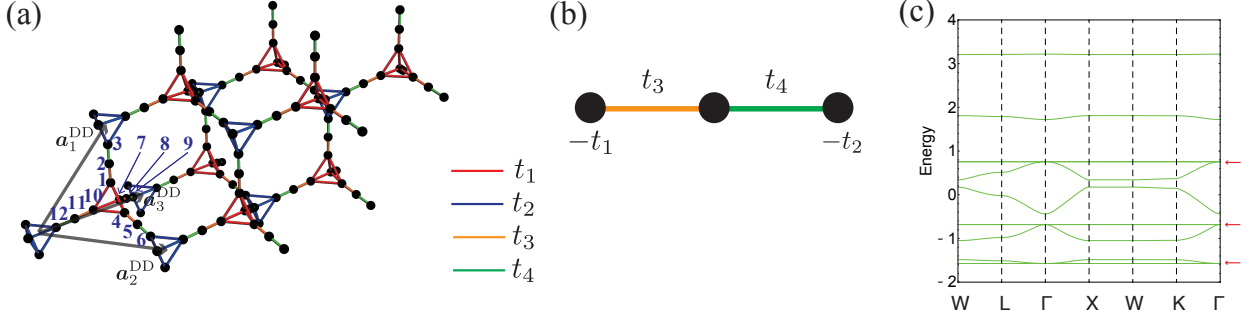


FIG. 8. (a) A decorated pyrochlore lattice with one decorated site between neighboring tetrahedra. (b) Schematic figure of the Hamiltonian of the chain-like molecule corresponding to $\mathcal{H}_{\text{linkage}}^{\text{DP}}$. (c) The band structure for $(t_1, t_2, t_3, t_4) = (1, 0.5, 0.8, 0.7)$. Red arrows point to the flat bands.

The j -th column of the second line of Eq. (34) is

$$\begin{aligned}
 & [\lambda_{\text{linker}, \mathbf{k}}]_j \tilde{\mathcal{H}}_{\text{linkage}}^{\text{DP}} + \sum_{j' \neq j} [\lambda_{\text{linker}, \mathbf{k}}]_{j'} \begin{pmatrix} t_1 & 0 & 0 \\ 0 & 0 & 0 \\ 0 & 0 & t_2 e^{-i\mathbf{k} \cdot (\mathbf{a}_j^{\text{DD}} - \mathbf{a}_{j'}^{\text{DD}})} \end{pmatrix} \\
 &= [\lambda_{\text{linker}, \mathbf{k}}]_j \left[\tilde{\mathcal{H}}_{\text{linkage}}^{\text{DP}} + \begin{pmatrix} -t_1 & 0 & 0 \\ 0 & 0 & 0 \\ 0 & 0 & -t_2 \end{pmatrix} \right] = [\lambda_{\text{linker}, \mathbf{k}}]_j \mathcal{H}_{\text{linkage}}^{\text{DP}}, \quad (35)
 \end{aligned}$$

which is equal to the j -th component of the right-hand side of Eq. (32). The second line of Eq. (35) can be obtained by using Eq. (8). Having Eq. (31) at hand, we again see that the flat-band eigenenergies are equal to those of $\mathcal{H}_{\text{linkage}}^{\text{DP}}$, and that the wave function of n th flat band is given as

$$\varphi_{3(j-1)+m, \mathbf{k}, n}^{\text{DP}} = \frac{1}{\mathcal{N}_{\mathbf{k}}} [\lambda_{\text{linker}, \mathbf{k}}]_j [\phi_{\text{linkage}, n}^{\text{DP}}]_m, \quad (36)$$

($j = 1, 2, 3, 4$, $m = 1, 2, 3$), where $\phi_{\text{linkage}, n}^{\text{DP}}$ is the eigenvector of $\mathcal{H}_{\text{linkage}}^{\text{DP}}$ corresponding to the n th eigenvalue. The corresponding molecule for $\mathcal{H}_{\text{linkage}}^{\text{DP}}$ is depicted in Fig. 8(b). Comparing $\tilde{\mathcal{H}}_{\text{linkage}}^{\text{DP}}$ with $\mathcal{H}_{\text{linkage}}^{\text{DP}}$, one finds that the on-site potentials, $-t_1$ and $-t_2$, are added at the end sites.

The band structure for a certain set of parameters is shown in Fig. 8(c). We obtain three flat bands, each of which is doubly degenerate. As we have discussed, their energies are equal to the eigenvalues of $\mathcal{H}_{\text{linkage}}^{\text{DP}}$.

V. SUMMARY AND DISCUSSIONS

We have presented the method to determine the flat-band energies and wave functions analytically in the decorated diamond lattices in arbitrary dimensions. The key idea is to divide the Hamiltonian into the linker part and the linkage part. Namely, by using the intertwiner [Eq. (11)] which is composed of the wave functions at

the linker, we can reduce the eigenvalue problem of \mathbf{k} -dependent $[(D+1)q+2] \times [(D+1)q+2]$ matrix ($\mathcal{H}_{\mathbf{k}}$) to the \mathbf{k} -independent $q \times q$ linkage Hamiltonian ($\mathcal{H}_{\text{linkage}}$). Further, we also find that the flat-band wave function of the D -dimensional decorated diamond lattice is given by the product of the linkage wave function and the flat-band wave function for the D -dimensional pyrochlore lattice.

We show the examples of the decorated honeycomb lattice in two dimensions, the decorated diamond lattice in three dimensions, and the decorated four-dimensional diamond lattice, where each NN bond is decorated by the chain-like structure. The condition for the multiple band touching at Γ point is also addressed. Further, the same method is applicable to the D -dimensional decorated pyrochlore lattices. There, the tetrahedral parts of the original Hamiltonian turn into the on-site potential at the edges of the linkage Hamiltonian.

In Sec. II, we have made several assumptions on the model in order to make the model relevant to real materials. However, from the theoretical viewpoint, some of the assumptions can be relaxed. The first extension is about the connection to the linkers and the linkages. We assume that each linkage is connected to the linker through one of the sites. However, this method can be used even when the linkage is connected to the linker with more than two sites. This is because an appropriate unitary transformation in the linkage part allows us to rewrite the model such that the linkage is connected to the linker by one “orbital”. The second extension is about the forms of the linkages. We assume that all the

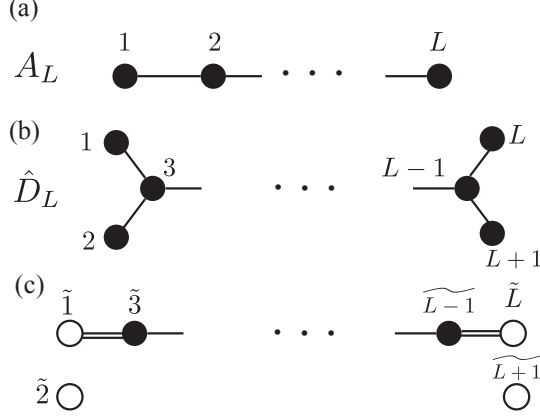


FIG. 9. The Dynkin diagram of (a) A_L and the extended Dynkin diagram of (b) \hat{D}_L . (c) Schematic figure of the chain plus two isolated sites equivalent to \hat{D}_L under the change of the basis. The single lines denote the bonds with the hopping being unity, while the double lines denote the bonds with the hopping being $\sqrt{2}$.

linkages have the same structure. However, our construction of the flat bands works even when each linkage has a different structure as far as the linkages have common eigenenergies.

To conclude, there are a number of materials with decorated honeycomb, diamond and pyrochlore lattice structures, especially for organic materials. We hope that our method to determine flat-band energies and wave functions is useful for band structure analysis and material design.

Note added.— Recently, we became aware of the related works [89, 90] where the flat bands of the decorated honeycomb model are discussed.

ACKNOWLEDGMENTS

This work is supported by JSPS KAKENHI, Grants No. JP17H06138 (T. M. and Y. H.) and No. JP20K14371 (T. M.). H. K. was supported in part by JSPS Grant-in-Aid for Scientific Research on Innovative Areas No. JP20H04630, JSPS KAKENHI Grant No. JP18K03445, and the Inamori Foundation.

Appendix A: Specific cases with triple band touching

In this appendix, we elucidate that the condition for the triple band touching at Γ point in the decorated honeycomb model can be found exactly for the special case. Specifically, we restrict ourselves to the case where $U_A = U_B = U_1 = \dots = U_q = 0$, $t_2 = \dots = t_q = 1$, and $t_1 = t_{q+1} = \tilde{t}$. The aim here is to determine \tilde{t} such that

all of the q flat bands are involved in triple band touching at Γ point, as shown in Fig. 3(f).

To this aim, we employ the wisdom of the eigenvalues of the adjacency matrices of the Dynkin diagrams (or A-D-E lattices). Specifically, for the present purpose, we consider the A type [Fig. 9(a)], which is nothing but the open chain, and the \hat{D} type [Fig. 9(b)], which has double branches at both ends. It is known [91, 92] that the eigenvalues of the adjacency matrix of A_L are given as

$$\varepsilon^{A_L} = 2 \cos \frac{j\pi}{L+1} \quad (j = 1, \dots, L), \quad (\text{A1})$$

while those of \hat{D}_L are given as

$$\varepsilon^{\hat{D}_L} = 0, 2 \cos \frac{j\pi}{L-2} \quad (j = 0, \dots, L-2). \quad (\text{A2})$$

From Eqs. (A1) and (A2), we see that all of the eigenvalues for A_L are included in the set of the eigenvalues of \hat{D}_{L+3} . We note that this fact can also be derived by explicitly giving the intertwiner between the adjacency matrices for these graphs. Namely, the following relation holds:

$$H_{\hat{D}_{L+3}} C_L = C_L H_{A_L}, \quad (\text{A3})$$

with

$$(C_L)_{ij} = \delta_{i,1}\delta_{j,1} + \delta_{i,j+1} - \delta_{i,j+3} - \delta_{i,L+4}\delta_{j,L} \quad (i = 1, \dots, L+4, j = 1, \dots, L), \quad (\text{A4})$$

where $H_{\hat{D}_{L+3}}$ and H_{A_L} stand for the adjacency matrices of \hat{D}_{L+3} and A_L , respectively.

Further, as for \hat{D}_L , by changing the basis as $|\tilde{1}\rangle = \frac{1}{\sqrt{2}}[|1\rangle + |2\rangle]$, $|\tilde{2}\rangle = \frac{1}{\sqrt{2}}[|1\rangle - |2\rangle]$, $|\tilde{L}\rangle = \frac{1}{\sqrt{2}}[|L\rangle + |L+1\rangle]$, $|\tilde{L+1}\rangle = \frac{1}{\sqrt{2}}[|L\rangle - |L+1\rangle]$, and $|\tilde{\ell}\rangle = |\ell\rangle$ ($\ell = 3, \dots, L-1$), where $|\ell\rangle$ denotes the state localized at the ℓ th site in the original graph, one can see that the hopping problem on the graph \hat{D}_L is equivalent to that on the $L-1$ -site chain where the hoppings on the both of the ends are modulated from 1 to $\sqrt{2}$ [see the double lines in Fig. 9(c)].

Combining these facts, we find the following: All of the eigenenergies of the q -site chain with the NN hopping being 1 are included in the set of the eigenenergies of the $q+2$ -site chain where the hoppings are $\sqrt{2}$ on the both of the ends and 1 otherwise. Turning to our original problem, we find that the multiple triple band touchings can be found by setting $\sqrt{3}\tilde{t} = \sqrt{2}$, which leads to $\tilde{t} = \sqrt{\frac{2}{3}}$. This is indeed the parameters employed for Fig. 3(f) (for $q = 3$). It is to be stressed that the condition for \tilde{t} obtained here is regardless of q . In fact, for $q = 2$, the multiple triple band touchings were found in Ref. 68 for the same parameter choice. We also note that, for D -dimensional systems, the multiple band touchings whose degeneracy is $D+1$ can be found for $\tilde{t} = \sqrt{\frac{2}{D+1}}$. An example of $D = 3$ is shown in Fig. 6(d).

Appendix B: High symmetry points of the first Brillouin zone in the four-dimensional diamond lattice

The four lattice vectors of the four-dimensional diamond lattice are

$$\mathbf{a}_1^{4DD} = \left(\frac{\sqrt{5}}{4}, \frac{\sqrt{5}}{4}, \frac{\sqrt{5}}{4}, \frac{5}{4} \right), \quad (\text{B1})$$

$$\mathbf{a}_2^{4DD} = \left(\frac{\sqrt{5}}{4}, -\frac{\sqrt{5}}{4}, -\frac{\sqrt{5}}{4}, \frac{5}{4} \right), \quad (\text{B2})$$

$$\mathbf{a}_3^{4DD} = \left(-\frac{\sqrt{5}}{4}, -\frac{\sqrt{5}}{4}, \frac{\sqrt{5}}{4}, \frac{5}{4} \right), \quad (\text{B3})$$

and

$$\mathbf{a}_4^{4DD} = \left(-\frac{\sqrt{5}}{4}, \frac{\sqrt{5}}{4}, -\frac{\sqrt{5}}{4}, \frac{5}{4} \right). \quad (\text{B4})$$

For the coordinates of the high-symmetry points in the first Brillouin zone in the four-dimensional diamond lat-

tice, we follow Ref. 83:

$$\Gamma = (0, 0, 0, 0), \quad (\text{B5})$$

$$\gamma_1 = \left(0, 0, 0, -\frac{4\pi}{5} \right), \quad (\text{B6})$$

$$\gamma_2 = \left(\frac{2\pi}{\sqrt{5}}, 0, 0, -\frac{2\pi}{5} \right), \quad (\text{B7})$$

$$L_1 = \left(\frac{4\pi}{5\sqrt{5}}, -\frac{4\pi}{5\sqrt{5}}, \frac{4\pi}{5\sqrt{5}}, -\frac{4\pi}{5} \right), \quad (\text{B8})$$

$$L_2 = \left(\frac{2\pi}{\sqrt{5}}, -\frac{2\pi}{5\sqrt{5}}, \frac{2\pi}{5\sqrt{5}}, -\frac{2\pi}{5} \right), \quad (\text{B9})$$

$$L_3 = \left(\frac{4\pi}{5\sqrt{5}}, \frac{4\pi}{5\sqrt{5}}, \frac{4\pi}{5\sqrt{5}}, -\frac{4\pi}{5} \right), \quad (\text{B10})$$

$$W_1 = \left(\frac{8\pi}{5\sqrt{5}}, 0, \frac{4\pi}{5\sqrt{5}}, -\frac{4\pi}{5} \right), \quad (\text{B11})$$

$$K_1 = \left(\frac{6\pi}{5\sqrt{5}}, 0, \frac{6\pi}{5\sqrt{5}}, -\frac{4\pi}{5} \right), \quad (\text{B12})$$

$$X_1 = \left(\frac{8\pi}{5\sqrt{5}}, 0, 0, -\frac{4\pi}{5} \right), \quad (\text{B13})$$

$$U_1 = \left(\frac{8\pi}{5\sqrt{5}}, -\frac{2\pi}{5\sqrt{5}}, \frac{2\pi}{5\sqrt{5}}, -\frac{4\pi}{5} \right), \quad (\text{B14})$$

$$U_2 = \left(\frac{8\pi}{5\sqrt{5}}, \frac{2\pi}{5\sqrt{5}}, \frac{2\pi}{5\sqrt{5}}, -\frac{4\pi}{5} \right). \quad (\text{B15})$$

-
- [1] O. Vafek and A. Vishwanath, *Annu. Rev. Condens. Matter Phys.* **5**, 83 (2014).
 - [2] N. P. Armitage, E. J. Mele, and A. Vishwanath, *Rev. Mod. Phys.* **90**, 015001 (2018).
 - [3] A. Bernevig, H. Weng, Z. Fang, and X. Dai, *J. Phys. Soc. Jpn.* **87**, 041001 (2018).
 - [4] K. S. Novoselov, E. McCann, S. V. Morozov, V. I. Fal'ko, M. I. Katsnelson, U. Zeitler, D. Jiang, F. Schedin, and A. K. Geim, *Nat. Phys.* **2**, 177 (2006).
 - [5] K. Fukushima, D. E. Kharzeev, and H. J. Warringa, *Phys. Rev. D* **78**, 074033 (2008).
 - [6] A. A. Zyuzin, S. Wu, and A. A. Burkov, *Phys. Rev. B* **85**, 165110 (2012).
 - [7] H. Fukuyama and R. Kubo, *J. Phys. Soc. Jpn.* **28**, 570 (1970).
 - [8] M. Koshino and T. Ando, *Phys. Rev. B* **76**, 085425 (2007); *Phys. Rev. B* **81**, 195431 (2010).
 - [9] A. Raoux, F. Piéchon, J.-N. Fuchs, and G. Montambaux, *Phys. Rev. B* **91**, 085120 (2015).
 - [10] H. Maebashi, M. Ogata, and H. Fukuyama, *J. Phys. Soc. Jpn.* **86**, 083702 (2017).
 - [11] J. V. von Neumann and E. Wigner, *Physik Z.* **30**, 467 (1929).
 - [12] Y. Hatsugai, *N. J. Phys.* **12**, 065004 (2010).
 - [13] K. Asano and C. Hotta, *Phys. Rev. B* **83**, 245125 (2011).
 - [14] A. Mielke, *J. Phys. A: Math. Gen.* **24** L73 (1991); *J. Phys. A: Math. Gen.* **24** 3311 (1991).
 - [15] H. Tasaki, *Phys. Rev. Lett.* **69**, 1608 (1992).
 - [16] A. Mielke and H. Tasaki, *Commun. Math. Phys.* **158**, 341 (1993).
 - [17] K. Kusakabe and H. Aoki, *Phys. Rev. Lett.* **72**, 144 (1994).
 - [18] H. Tasaki, *Prog. Theor. Phys.* **99**, 489 (1998).
 - [19] K. Tamura and H. Katsura, *Phys. Rev. B* **100**, 214423 (2019).
 - [20] H. Tasaki, *Physics and Mathematics of Quantum Many-Body Systems*, Springer, Berlin (2020).
 - [21] M. Imada and M. Kohno, *Phys. Rev. Lett.* **84**, 143 (2000).
 - [22] K. Kuroki, T. Higashida, R. Arita, *Phys. Rev. B* **72**, 212509 (2005).
 - [23] K. Kobayashi, M. Okumura, S. Yamada, M. Machida, and H. Aoki, *Phys. Rev. B* **94**, 214501 (2016).
 - [24] K. Matsumoto, D. Ogura, and K. Kuroki, *Phys. Rev. B* **97**, 014516 (2018).
 - [25] H. Aoki, *Journal of Superconductivity and Novel Magnetism* **33**, 2341 (2020).
 - [26] H. Aoki, M. Ando, and H. Matsumura, *Phys. Rev. B* **54**, R17296(R) (1996).
 - [27] J. Vidal, R. Mosseri, and B. Douçot, *Phys. Rev. Lett.* **81**, 5888 (1998).
 - [28] H. M. Guo and M. Franz, *Phys. Rev. B* **80**, 113102 (2009).
 - [29] C. Weeks and M. Franz, *Phys. Rev. B* **82**, 085310 (2010).
 - [30] H. Katsura, I. Maruyama, A. Tanaka, and H. Tasaki, *Europhys. Lett.* **91** 57007 (2010).
 - [31] D. Green, L. Santos, and C. Chamon, *Phys. Rev. B* **82**, 075104 (2010).
 - [32] E. Tang, J.-W. Mei, and X.-G. Wen, *Phys. Rev. Lett.* **106**, 236802 (2011).

- [33] K. Sun, Z. Gu, H. Katsura, and S. Das Sarma, Phys. Rev. Lett. **106** 236803 (2011).
- [34] T. Neupert, L. Santos, C. Chamon, and C. Mudry, Phys. Rev. Lett. **106**, 236804 (2011).
- [35] D. N. Sheng, Z.-C. Gu, K. Sun, and L. Sheng, Nat. Commun. **2**, 389 (2011).
- [36] F. Wang and Y. Ran, Phys. Rev. B **84**, 241103(R) (2011).
- [37] Z. Liu, E. J. Bergholtz, H. Fan, and A. M. Läuchli, Phys. Rev. Lett. **109**, 186805 (2012).
- [38] B. Pal, Phys. Rev. B **98**, 245116 (2018).
- [39] J. W. Rhim and B.-J. Yang, Phys. Rev. B **99**, 045107 (2019).
- [40] T. Mizoguchi and Y. Hatsugai, Phys. Rev. B **101**, 235125 (2020).
- [41] Y. Kuno, Phys. Rev. B **101**, 184112 (2020).
- [42] Y. Kuno, T. Mizoguchi, and Y. Hatsugai, Phys. Rev. A **102**, 063325 (2020).
- [43] M. Goda, S. Nishino, and H. Matsuda, Phys. Rev. Lett. **96**, 126401 (2006).
- [44] J. T. Chalker, T. S. Pickles, and P. Shukla, Phys. Rev. B **82**, 104209 (2010).
- [45] T. Bilitewski and R. Moessner, Phys. Rev. B **98**, 235109 (2018).
- [46] Y. Kuno, T. Orito, and I. Ichinose, N. J. Phys. **22**, 013032 (2020).
- [47] C. Danieli, A. Andreanov, and S. Flach, Phys. Rev. B **102**, 041116(R) (2020).
- [48] T. Orito, Y. Kuno, and I. Ichinose, Phys. Rev. B **103**, L060301 (2021).
- [49] B. Sutherland, Phys. Rev. B **34**, 5208 (1986).
- [50] S. Miyahara, K. Kubo, H. Ono, Y. Shimomura, and N. Furukawa, J. Phys. Soc. Jpn. **74**, 1918 (2005).
- [51] Y. Hatsugai and I. Maruyama, Europhys. Lett. **95**, 20003 (2011).
- [52] W. Maimaiti, A. Andreanov, H. C. Park, O. Gendelman, and S. Flach, Phys. Rev. B **95**, 115135 (2017).
- [53] T. Misumi and H. Aoki, Phys. Rev. B **96**, 155137 (2017).
- [54] W. Maimaiti, S. Flach, and A. Andreanov, Phys. Rev. B **99**, 125129 (2019).
- [55] T. Mizoguchi and M. Udagawa, Phys. Rev. B **99**, 235118 (2019).
- [56] T. Mizoguchi and Y. Hatsugai, Europhys. Lett. **127**, 47001 (2019).
- [57] C.-C. Lee, A. Fleurence, Y. Yamada-Takamura, and T. Ozaki, Phys. Rev. B **100**, 045150 (2019).
- [58] W. Maimaiti, A. Andreanov, and S. Flach, arXiv:2101.03794.
- [59] Y. Hatsugai, K. Shiraishi, and H. Aoki, N. J. Phys. **17**, 025009 (2015).
- [60] Y. Fujii, M. Maruyama, and S. Okada, Jpn. J. Appl. Phys. **57**, 125203 (2018).
- [61] Y. Fujii, M. Maruyama, and S. Okada, Jpn. J. Appl. Phys. **58**, 085001 (2019).
- [62] T. Mizoguchi, M. Maruyama, S. Okada, and Y. Hatsugai, Phys. Rev. Mater. **3**, 114201 (2019).
- [63] N. Shima and H. Aoki, Phys. Rev. Lett. **71**, 4389 (1993).
- [64] N. Morishita and K. Kusakabe, arXiv:2102.03835.
- [65] R. H. Baughman, H. Eckhardt, and M. Kertesz, J. Chem. Phys. **87**, 6687 (1987).
- [66] R. Longuinhos, E. A. Moujaes, S. S. Alexandre, and R. W. Nunes, Chem. Mater. **26**, 3701 (2014).
- [67] Z. Li, M. Smeu, A. Rives, V. Maraval, R. Chauvin, M. A. Ratner, and E. Borguet, Nat. Commun. **6**, 6321 (2015).
- [68] C. Barreateau, F. Ducastelle, and T. Mallah, J. Phys.: Condens. Matter **29**, 465302 (2017).
- [69] Z. Liu, Z.-F. Wang, J.-W. Mei, Y.-S. Wu, and F. Liu, Phys. Rev. Lett. **110**, 106804 (2013).
- [70] M. G. Yamada, T. Soejima, N. Tsuji, D. Hirai, M. Dincă, and H. Aoki, Phys. Rev. B **94**, 081102(R) (2016).
- [71] A. Kumar, K. Banerjee, A. S. Foster, and P. Liljeroth, Nano Lett. **18**, 5596 (2018).
- [72] J. M. Lee, C. Geng, J. W. Park, M. Oshikawa, S.-S. Lee, H. W. Yeom, and G. Y. Cho, Phys. Rev. Lett. **124**, 137002 (2020).
- [73] J. W. Park, G. Y. Cho, J. Lee, and H. W. Yeom, Nat. Commun. **10**, 4038 (2019).
- [74] T. Mizoguchi, Y. Kuno, and Y. Hatsugai, Phys. Rev. A **102**, 033527 (2020).
- [75] T. Mizoguchi, T. Yoshida, and Y. Hatsugai, Phys. Rev. B **103**, 045136 (2021).
- [76] H. Katsura and I. Maruyama, Kotai Butsuri **50**, 257-269 (2015) (in Japanese).
- [77] J.-Y. You, B. Gu, and G. Su, Sci. Rep. **9**, 20116 (2019).
- [78] Note that Ψ_k^\dagger was called the “molecular orbital” (MO) for the D -dimensional pyrochlore model [51], by which the Hamiltonian of the tight-binding model with NN hoppings being t can be written as $\mathcal{H}_k^{\text{Py}} = t [\Psi_k \Psi_k^\dagger - 2I_{D+1}]$, with I_{D+1} being the $(D+1) \times (D+1)$ identity matrix.
- [79] P. Di Francesco and J.-B. Zuber, Nucl. Phys. B **338**, 602 (1990).
- [80] P. A. Pearce and Y.-K. Zhou, Int. J. Mod. Phys. B **7**, 3649 (1993).
- [81] M. Creutz, JHEP **04**, 017 (2008).
- [82] T. Kimura and T. Misumi, Prog. Theor. Phys. **123**, 63 (2010); *ibid.* **124**, 415 (2010).
- [83] Y. Kato and M. Yamanaka, J. Phys. Soc. Jpn. **86**, 033601 (2017).
- [84] F. D. M. Haldane, Phys. Rev. Lett. **61**, 2015 (1988).
- [85] T. Fukui, Y. Hatsugai, and H. Suzuki, J. Phys. Soc. Jpn. **74**, 1674 (2005).
- [86] X.-L. Sheng, Q.-B. Yan, F. Ye, Q.-R. Zheng, and G. Su, Phys. Rev. Lett. **106**, 155703 (2011).
- [87] C. Janani, J. Merino, I. P. McCulloch, and B. J. Powell, Phys. Rev. Lett. **113**, 267204 (2014).
- [88] C. Peng, Y. Xie, Z. Zhang, and Y. Chen, International Journal of Heat and Mass Transfer **164**, 120483 (2021).
- [89] Z. Qi, E. Bobrow, and Y. Li, arXiv:2012.07806.
- [90] N. Boudjada, F. L. Buessen, and A. Paramekanti, arXiv:2012.07847.
- [91] A. E. Brouwer and W. H. Haemers, *Spectra of Graphs*, Springer, New York (2012).
- [92] M. Henkel, *Conformal Invariance and Critical Phenomena*, Springer, Berlin Heidelberg (1999).